ORIGINAL RESEARCH

Cardiac Overexpression of S100A6 Attenuates Cardiomyocyte Apoptosis and Reduces Infarct Size After Myocardial Ischemia-Reperfusion

Azadeh Mofid, MD, PhD; Nadav S. Newman, BA, BSc; Paul J. H. Lee, MSc; Cynthia Abbasi, MSc; Pratiek N. Matkar, MSc; Dmitriy Rudenko, BSc; Michael A. Kuliszewski, BSc; Hao H. Chen, MSc; Kolsoom Afrasiabi, MD; James N. Tsoporis, PhD; Anthony O. Gramolini, PhD; Kim A. Connelly, MBBS, PhD; Thomas G. Parker, MD, PhD; Howard Leong-Poi, MD

***Background*—**Cardiomyocyte-specific transgenic mice overexpressing S100A6, a member of the family of EF-hand calcium-binding proteins, develop less cardiac hypertrophy, interstitial fibrosis, and myocyte apoptosis after permanent coronary ligation, findings that support S100A6 as a potential therapeutic target after acute myocardial infarction. Our purpose was to investigate S100A6 gene therapy for acute myocardial ischemia-reperfusion.

***Methods and Results*—**We first performed in vitro studies to examine the effects of S100A6 overexpression and knockdown in rat neonatal cardiomyocytes. S100A6 overexpression improved calcium transients and protected against apoptosis induced by hypoxia-reoxygenation via enhanced calcineurin activity, whereas knockdown of S100A6 had detrimental effects. For in vivo studies, human S100A6 plasmid or empty plasmid was delivered to the left ventricular myocardium by ultrasound-targeted microbubble destruction in Fischer-344 rats 2 days prior to a 30-minute ligation of the left anterior descending coronary artery followed by reperfusion. Control animals received no therapy. Pretreatment with S100A6 gene therapy yielded a survival advantage compared to empty-plasmid and nontreated controls. S100A6-pretreated animals had reduced infarct size and improved left ventricular systolic function, with less myocyte apoptosis, attenuated cardiac hypertrophy, and less cardiac fibrosis.

***Conclusions*—**S100A6 overexpression by ultrasound-targeted microbubble destruction helps ameliorate myocardial ischemia-reperfusion, resulting in lower mortality and improved left ventricular systolic function post–ischemia-reperfusion via attenuation of apoptosis, reduction in cardiac hypertrophy, and reduced infarct size. Our results indicate that S100A6 is a potential therapeutic target for acute myocardial infarction. **(*J Am Heart Assoc*. 2017;6:e004738. DOI: 10.1161/JAHA.116.004738.)**

Key Words: apoptosis • gene therapy • hypertrophy • ischemia-reperfusion • S100A6 • ultrasound-targeted microbubble destruction

Early reperfusion by thrombolytic therapy or percutaneous coronary intervention limits infarct size and reduces mortality in patients presenting with acute ST-segment elevation myocardial infarction.[1,2] Although outcomes have improved, morbidity and mortality still remain significant, with in-hospital mortality rates of 3% to 4%,[3] 30-day mortality rates of 5% to 7%,[4] 3-year rates of major adverse cardiovascular events ranging from 16% to 17%,[5] and 30-day rehospitalization rates of 15% to 20%.[6] Although essential, the acute restoration of blood flow within the epicardial coronary artery can lead to metabolic and structural events that result in a further loss of cardiomyocytes through multiple mechanisms, termed myocardial ischemia-reperfusion (I/R) injury.[7,8] As a consequence, the development of new therapies to further reduce infarct size and preserve left ventricular (LV) systolic function after acute ST-segment elevation myocardial infarction remains a priority.[9–11]

Myocardial I/R injury is a complex, multifaceted process that has been extensively studied, with important contributing factors from oxidative stress, calcium overload, immune responses, inflammation, and impaired metabolism, leading to myocyte and endothelial cell loss by several mechanisms including apoptosis, necrosis, and autophagy.[7,9] Thus, the ability to specifically target multiple underlying biologic

From the Division of Cardiology, Keenan Research Centre for Biomedical Science, Li Ka Shing Knowledge Institute, St. Michael's Hospital (A.M., N.S.N., P.J.H.L., P.N.M., D.R., M.A.K., H.H.C., K.A., J.N.T., K.A.C., T.G.P., H.L.-P.) and Department of Physiology (C.A., A.O.G.), University of Toronto, Ontario, Canada.

Correspondence to: Howard Leong-Poi, MD, FRCPC, FASE, FACC, 6-044 Donnelly Wing, St. Michael's Hospital, 30 Bond Street, Toronto, Ontario, Canada M5B 1W8. E-mail: leong-poih@smh.ca

Received September 23, 2016; accepted January 4, 2017.

processes involved in reperfusion injury would be a key aspect in the development of novel therapeutic strategies to address myocardial I/R.

S100A6 is a member of a superfamily of EF-hand Ca^{2+}-binding proteins that regulate a wide array of cellular and molecular functions, including cell proliferation, differentiation, and survival as well as Ca^{2+} dynamics, cardiomyocyte contractility, hypertrophy, and apoptosis.[12] S100A6 expression is increased in the heart after MI[13] and inhibits the induction of the cardiac fetal gene promoters in cultured neonatal rat cardiac myocytes in vitro,[14] which suggests that it plays a role in modulating cardiac hypertrophy. Overexpression of S100A6 in vitro prevented cardiomyocyte apoptosis induced by tumor necrosis factor-α by interfering with p53 phosphorylation.[15] Most recently, cardiac myocyte-specific transgenic mice overexpressing S100A6 showed attenuation of cardiac hypertrophy, less interstitial fibrosis, and reduced myocyte apoptosis compared to control animals in a permanent coronary ligation model of MI.[16]

Given that S100A6 has the potential to modulate several key pathways involved in I/R injury, including myocyte apoptosis and Ca^{2+} dynamics, as well as positively influence cardiac hypertrophy, a key element in the remodeling process post-MI, we hypothesized that gene transfer of S100A6 would ameliorate myocardial reperfusion injury and attenuate LV systolic dysfunction in a rat model of I/R. The present study demonstrates that the mechanisms of S100A6 therapy in the setting of myocardial I/R are multifactorial, with effects on cardiomyocytes to reduce apoptosis, attenuate hypertrophy, and increase Ca^{2+} cycling. These findings, coupled with the positive data from transgenic mice,[16] support S100A6 as a novel therapeutic target for acute myocardial I/R.

Methods

Neonatal Rat Cardiomyocyte Isolation and Purification

Rat neonatal ventricular myocytes (NRVM) from 2- to 3-day-old Fisher 344 rats (Charles River Laboratories International, Wilmington, MA) were isolated using a Worthington Neonatal Cardiomyocyte Isolation system (Worthington Biochemical Corporation, Lakewood, NJ; catalog #LK003303), according to the manufacturer's protocol. In brief, 2- to 3-day-old rat pups were sacrificed by decapitation. After sterilization, the beating hearts were surgically removed and immediately placed in centrifuge tubes containing 30 to 40 mL of sterile calcium-magnesium–free Hanks Balanced Salt Solution (CMF HBSS, pH 7.4, Reagent 1) to chill and rinse. The tissue was minced with small scissors to less than 1 mm^3 pieces while being kept at 0°C and then incubated overnight (16-20 hours) at 2°C to 8°C in 10 mL of CMF HBSS containing purified trypsin (Reagent 2) at a final concentration of 50 μg/mL.

After the incubation time, tissue and buffer were mixed with trypsin inhibitor (Reagent 3) and oxygenated for 30 seconds by passing oxygen over the surface of the liquid. Tissue and buffer were warmed to 30°C to 37°C in a water bath, and collagenase (Reagent 4) was added, followed by incubation for 30 to 45 minutes at 37°C on a slowly rotating or shaking instrument. The tubes were removed from the incubator, cells released by triturating 10 times using standard 10 mL plastic serological pipettes, and then filtered through the cell strainer into a fresh 50-mL centrifuge tube. Cells were sedimented at 180*g* for 5 minutes, and the final cell pellet was suspended in Dulbecco Modified Eagle Medium: Nutrient Mixture F-12 (DMEM/F-12) (Life Technologies, Carlsbad, CA; catalog #11320-033) growth medium containing 7.5% horse serum (Life Technologies, catalog #16050-130), 7.5% fetal bovine serum (Life Technologies, catalog #26140-079), and 100 U/mL penicillin with 100 μg/mL streptomycin (Life Technologies, catalog #15140122). The cells were plated for 1.5 to 2 hours to allow the differential attachment of nonmyocardial cells (mostly fibroblasts). The nonadhesive cells (cardiomyocytes) were transferred to a centrifugation tube, washed, and centrifuged again at 180*g* for 5 minutes. After counting, the myocyte-enriched suspension was transferred to collagen I–coated culture dishes at density of 5×10^4 cells/cm^2. The viability of cells (85% to 90%) was determined by exclusion of trypan blue dye. Cells were incubated in 95% air and 5% CO_2 at 37°C and left untouched for at least 48 hours.

In Vitro Transduction and Adenoviral Vectors

Cultured neonatal rat cardiomyocytes (5×10^4/cm^2 cells grown for 48 hours after seeding), were inoculated with Ad-CMV-Null (2.25×10^{10} PFU/mL, MOI:100), Ad-CMV-emGFP-hS100A6 (2.8×10^9 PFU/mL, MOI:100), and Ad-GFP-U6-rS100A6-shRNA (4.0×10^{10} PFU/mL, MOI:100) adenoviral vectors in 250 μL/cm^2 of serum containing 7% Horse serum plus 7% fetal bovine serum DMEM/F12 growth medium (Life Technologies, catalog #11330-032) for 24 hours. All adenoviral vectors were constructed in Vector BioLabs (Malvern, PA).

shRNA sequence (TRCN0000087874): CCGG-GCTTTGATCTACAATGAAGCT-CTCGAG-AGCTTCATTGTAGATCAAAGC-TTTTTG

Target sequence: GCTTTGATCTACAATGAAGCT

Hairpin sequence: CTCGAG

The virus-containing growth medium was replaced with fresh medium after 24 hours, but cells were incubated for another 24 hours to have maximal expression of overexpressed gene (human S100A6) and downregulation of knocked-down gene (rat S100A6) at the time of hypoxia/reoxygenation (H/R) induction or calcium transient studies.

Real-Time Quantitative Polymerase Chain Reaction

Total RNA was extracted using Trizol reagent, and reverse-transcribed into cDNA using a reverse transcription system. Polymerase chain reaction (PCR) amplification was performed with Power SYBR Green PCR Master Mix in a StepOne. Gene expression levels were normalized with housekeeping gene rat TBP, and data were analyzed with StepOne software (Applied Biosystems, Foster City, CA) v2.1. The primers' sequences we used were as follows (Table).

Protein Extraction and Western Blotting

Tissue samples were homogenized and protein concentrations determined according to the method of Bradford protein assay. The proteins of equal loading were separated by sodium dodecyl sulfate polyacrylamide gel electrophoresis and transferred to a polyvinylidene difluoride membrane. Membranes were incubated with rabbit monoclonal anti-S100A6 antibody (Novus Biologicals, Littleton, CO; catalog #NBP1-95284) or rabbit polyclonal anti–green fluorescent protein (GFP) antibody (Abcam, Cambridge, UK; catalog #ab6556) and anti-rabbit IgG horseradish peroxidase–conjugated (Promega, Madison, WI; catalog #W401B). Blots of proteins were probed with rabbit polyclonal anti-GAPDH primary antibody (Santa Cruz Biotechnologies, Dallas, TX; catalog #sc-25778) for internal reference. Secondary antibodies were detected using Immobilon Western chemiluminescence horseradish peroxidase substrate (Millipore, Billerica, MA; catalog #WBKLS0050). Band intensity was quantified by scanning densitometry using a VersaDoc Imaging System (Bio-Rad, Hercules, CA).

Table. Primers' sequence

Rats S100A6 primer:
5′-GGCCATCGGCCTTCTCGTGG-3′ (forward)
5′-TGCTCAGGGTGTGCTTGTCACC-3′ (reverse)
Rat TBP primer:
5′-CCATTGCCAGGCACCACCCC-3′ (forward)
5′-AGGCTGGTGTGGCAGGAGTGA-3′ (reverse)
Rat S100B primer:
5′-GGAGCTCATCAACAACGAGC-3′ (forward)
5′-GGAAGTCACACTCCCCATCC-3′ (reverse)
Rat S100A1 primer:
5′-CAATGTGTTCCATGCCCACTC-3′ (forward)
5′-AGCAGGTCTTTCAGCTCCTTC-3′ (reverse)
Human/Rat S100A6 primer:
5′-GACAAGCACACCCTGAGCAA-3′ (forward)
5′-CAGCCTTGCAATTTCAGCATCC-3′ (reverse)
Rat β-myosin heavy chain (βMHC):
5′-GCCAACTATGCTGGAGCTGA-3′ (forward)
5′-GATTTTCCCTGTGCAGTGCG-3′ (reverse)
Rat Atrial natriuretic factor (ANF):
5′-CTGGACTGGGGAAGTCAACC-3′ (forward)
5′-GATCTATCGGAGGGGTCCCA-3′ (reverse)
CaN A:
5′-TCCGACGCCAACCTTAACTC-3′ (forward)
5′-GCTGCTATTACTGCCGTTGC-3′ (reverse)
CaN B:
5′-CCGTTCCTTTTCCCCCAACT -3′ (forward)
5′-AACCCTGGGTATCCCATCCA-3′ (reverse)

Hypoxia/Reoxygenation Induction In Vitro

Hypoxic conditions were created by incubating culture dishes in an airtight Plexiglas chamber with an atmosphere of 1% O_2, 20% CO_2, and 79% N_2 at 37°C for 24 hours. Serum-free low-glucose growth medium, Dulbecco Modified Eagle Medium, DMEM×1 (Life Technologies, Carlsbad, CA; catalog #11885-084) was preequilibrated in the hypoxic chamber overnight before use. Reperfusion/reoxygenation was simulated by returning the cultured cells to the incubator with an atmosphere of 95% air and 5% CO_2 at 37°C for 6 hours in serum containing DMEM/F12 medium.

Intracellular Calcium Transients During Spontaneous Action Potential

Neonatal cardiomyocytes were incubated in 0.5 μmol/L Fura-2AM in serum-free medium (DMEM/F12 medium+50 units penicillin/50 μg) for 1 hour and washed with serum-free medium. A fluorescence microscope (Olympus IX81, Tokyo, Japan; X-cite 120Q light source from EXFO, Quebec, QC, Canada; Fura 2B filterset from Semrock, Rochester, NY; using single-band excitation [387 nm] and single-band emission [510 nm], image acquisition with a Rolera MGi plus EM-CCD from Q-Imaging, Surrey, BC, Canada; via Metamorph v7.6.3. software, Nashville, TN) was used to acquire calcium transients.[17]

Immunocytochemistry and TUNEL Apoptotic Detection Assay

Neonatal cardiomyocytes were grown directly onto glass slides and transduced with adenoviral vectors for overexpression or knockdown of S100A6. H/R injury was created by incubating in the hypoxic incubation chamber followed by reoxygenation, as described above. Cells were washed twice with 1× phosphate-buffered saline and fixed in 2%

paraformaldehyde. Tissue sections were permeabilized in either 2:1 ratio solution of ethanol:acetic acid (for terminal deoxynucleotidyl transferase dUTP nick end labeling [TUNEL] slides) or 0.025% Triton X-100 for immunohistochemistry. Mouse monoclonal anti–cardiac troponin T antibody (Abcam, Cambridge, UK; catalog #ab10214), rabbit monoclonal anti-S100A6 antibody (Novus biologicals, Littleton, CO; catalog #NBP1-95284), goat anti–mouse IgG (Cy5) (Abcam, catalog #ab6563-100), and donkey antirabbit IgG (FITC) (GeneTex Inc, Irvine, CA; catalog #GTX26798) were used for immunostaining.

Neonatal cardiac myocytes cultured overnight were treated with vehicle (phosphate-buffered saline) (endogenous level) or with pure recombinant S100A6 protein tagged to His (Life Technologies, Carlsbad, CA) at a concentration of 100 nmol/L each for 1 hour. Cells were then fixed with 4% paraformaldehyde, permeabilized, and incubated with sheep anti-S100A6 (1:400, R&D) and rabbit anti-Histidase fusion protein (1:800, Abcam) followed by fluorochrome-conjugated secondary antibodies, donkey anti–sheep Alexa 488 (1:400) or chicken anti–rabbit Alexa 543 (1:400) (Molecular Probes, Eugene, OR), respectively. Extracellular protein uptake and subcellular localization were visualized by confocal microscopy. Images were generated with a Zeiss (Oberkochen, Germany) LSM 700 confocal laser scanning microscope using excitation wavelength of 488 nm and 543 nm for Alexa green and red dyes, respectively.

A subset of sections was also processed for apoptotic cell labeling using Apoptag Red in situ Apoptosis Detection kit (Millipore, Billerica, MA; catalog #2189979). The nuclei were counterstained with DAPI containing Vectashield mounting medium (Vector BioLabs, Malvern, PA; catalog #H1200).

Caspase 3/7 Activity Assay

Caspase 3/7 activity was measured using Caspase 3/7-Glo Assay (Promega, Madison, WI; catalog #G8091) by measuring the luminescence corresponding to the amount of caspase 3/7 activity from the total protein isolate. The luminescence was measured and quantified by a luminometer.

Calcineurin Phosphatase Activity Assay

A colorimetric assay kit was used to measure cellular CaN (PP2B) phosphatase activity (Enzo Life Science, Farmingdale, NY; catalog #BML-AK816-0001) in cellular extracts. Human recombinant CaN was included as a positive control.

Plasmid Preparation

An expression vector driven by a cytomegalovirus promoter was constructed for transfection of human S100A6-N-emGFP, in which the human S100A6 sequence was fused with emGFP at the N-terminus to create a fusion protein. GUS-N-eGFP was used as the empty plasmid for the control group. The plasmid vector was acquired through SIDNET (Toronto, ON, Canada) and was sequence-verified prior to use in vivo.

Ultrasound-Targeted Microbubble Destruction Gene Delivery

The study protocol was approved by the Animal Care and Use Committee at the Keenan Research Centre for Biomedical Science, St Michael's Hospital, University of Toronto, in accordance with the NIH Guide for the Care and Use of Laboratory Animals. Cationic lipid microbubbles (1×10^9) were charge-coupled to 500 μg of plasmid DNA (S100A6 or empty plasmid), as previously described. Under anesthesia, a cannula was placed in the rat's jugular vein for intravenous injections. For ultrasound-targeted microbubble destruction (UTMD), high-power ultrasound at a pulsing interval of 10 cardiac cycles at end-systole was transmitted to the LV via an S12 transducer (Sonos 5500, Philips Healthcare, Andover, MA) at a frequency of 5 MHz, 2 cm depth, power 120 V during intravenous infusion of plasmid-cationic microbubble complexes via the jugular vein over 5 minutes (Model AS50-Baxter).[18] The probe was positioned to cut the LV in a transverse plane (short-axis) at the midpapillary level, and the transducer was slowly moved from the base to the apex to allow maximal myocardial delivery.[18] Ultrasound transmission was continued for an additional 25 minutes after plasmid-microbubble infusion to ensure maximal delivery of remaining circulating DNA-microbubble complexes. Animals were subsequently given Anafen 5 mg/kg and placed on a warming pad at 37°C and allowed to recover.

Ischemia/Reperfusion Induction Surgery

Ischemia/reperfusion injury was induced via left anterior descending (LAD) coronary artery ligation for 30 minutes followed by reperfusion in Fischer-344 rats, at day 2 after UTMD (S100A6 or empty plasmid). Control animals did not receive UTMD prior to I/R. Animals were anesthetized with inhaled 2% to 5% isoflurane in 1.5 L/min oxygen, intubated, and volume-controlled ventilated (110/min with tidal volume of 0.25 mL) with 1.5% isoflurane in 1.5 L/min oxygen using a rodent respirator (model 683, Harvard Apparatus, Holliston, MA). The toe-pinch method was used to ensure the adequacy of anesthetic. Buprenorphine (0.02 mg/kg subcutaneously [SC]) and Anafen (5 mg/kg SC) were administered prior to the surgery. After preparation of the surgical site with alcohol and povidone-iodine, under sterile conditions, the rat's chest was opened. An incision was made in the skin on the left side of the chest, and the pectoral muscles were gently retracted to

expose the ribs. An incision was made through the fourth intercostal space, and the ribs were gently spread to expose the heart.

A curved needle was passed through the myocardium beneath the LAD coronary artery just below the atrial appendage. Ischemia was induced by ligation of LAD with a 6-0 prolene ligature. The suture was then routed into a clamping device, which would compress the artery to induce a reversible occlusion. The procedure was successful when myocardium changed color from a red hue to pale and white. After 30 minutes the clamp was released, and the ligature was removed. Reperfusion was confirmed by observing the change from cyanotic to pink in the myocardium. The chest was compressed to expel intrapleural air. The ribs, muscle, and skin were sutured, saline was administered (10 mL/kg SC), and the animals were ventilated using room air until spontaneous breathing resumed. After recovery they were extubated and placed on a warming blanket. Successful I/R induction was confirmed by echocardiography after surgery. Animals were followed out to day 28, with a subgroup sacrificed at day 1 post-I/R. Euthanasia was performed by means of cervical dislocation while under isoflurane-induced anesthesia. On sacrifice, tissue was harvested for postmortem analyses.

Risk Area Assessment by Evans Blue

Under anesthesia, a cannula was placed in the jugular vein for intravenous (IV) injections. LAD ligation was performed as described above. At 15 minutes after ligation, a 2% solution (4 mL) of Evans blue (Sigma, St. Louis, MO) was injected over 1 minute through the IV catheter. Five minutes after injection animals were sacrificed, the heart was removed, and 1-mm-thick transverse sections of the LV were cut distal to the ligation site. Sections were fixed in 10% buffered formalin for 48 hours and imaged (Olympus E1 Camera system, Tokyo, Japan). Images were processed in Image J, and risk area was quantified (nonperfused area/total LV area). Evans blue marked the perfused region during ligation, and the risk area was delineated by the non–Evans blue–stained myocardium.

Two-Dimensional Echocardiography

Under anesthesia (inhaled isoflurane anaesthetic, 0.2 L/min medical air, 3% isoflurane via nose cone), echocardiography was performed using Vevo® 2100 system (Visual Sonics, Toronto, ON, Canada) with an MS250 transducer (13-24 MHz) before surgery and 1, 2, 3, 7, 14, and 28 days after I/R injury. A parasternal long-axis view was recorded, ensuring that the mitral and aortic valves and the apex were visualized. A short-axis view was recorded at the level of the midpapillary muscles. Both 2-dimensional and motion-mode views were recorded at the same level. LV end-diastolic dimension, end-systolic dimension, fractional shortening, fractional area change, and the circumferential extent of the akinetic segment of the LV were measured from the short-axis view. LV ejection fraction was measured in parasternal long-axis view using a monoplane Simpson technique. All values were averaged over 3 consecutive cycles.

Cardiomyocyte Size and Myocyte Hypertrophy

The extent of cardiac myocyte hypertrophy was determined from hemotoxylin-eosin–stained sections. In brief, spindle-shaped cardiac myocytes with elliptical nuclei in a noninfarct region of transverse myocardial section were selected. The area of each cell was measured at the level of the nucleus using imaging software (NIS-Elements; Nikon, Tokyo, Japan), and the values were averaged. Approximately 3 cells per field at $\times 40$ magnification were found with 2 fields randomly selected per sample slide. Each treatment group included 10 animals and 10 slides. The average diameter of 50 to 60 myocytes was then calculated for 10 animals in each treatment group.

Triphenyl-Tetrazolium Chloride and Masson Trichrome Stain

We used 2,3,5-triphenyl-tetrazolium chloride (TTC) staining (Sigma-Aldrich, St. Louis, MO; catalog #T8877-10G) to define the nonviable/infarcted myocardium in LV myocardial slices at 24 hours post-I/R. We also used Masson Trichrome Stain Kit (Polysciences Inc, Warminster, PA; catalog #25088-100) to detect collagen fibers (stained blue) and necrotic tissue in the infarcted area of the LV myocardium (stained pink).

TUNEL Apoptosis Assay

Analysis of apoptosis was performed in 1 LV section per animal, obtained from the region that showed maximal infarct size. Using the ApopTag® Peroxidase In Situ Apoptosis Detection Kit (EMD Millipore, Darmstadt, Germany), apoptotic cardiomyocytes were detected through labeling and detecting DNA strand breaks by TUNEL (Millipore, Billerica, MA; catalog #S7160). The apoptotic index ($FITC^+$ nuclei$\times 100/DAPI^+$ nuclei) was calculated in various regions of LV sections using fluorescent microscopy with a magnification of $\times 40$. The density of cardiomyocyte nuclei was counted in at least 4 representative microscopic fields within each region of interest. The cardiomyocyte origin of the apoptotic cells was identified by immunohistochemical staining for α-actinin. The assay was standardized with the use of some sections treated with DNase I (1 U/mL for 30 minutes at 37°C) to induce the formation of DNA strand breaks (positive control of apoptosis).

Statistical Analysis

Continuous variables are presented as mean±SEM, and categorical data are summarized as frequencies or percentages. For categorical variables, differences between groups are evaluated with chi-squared test followed by Bonferroni correction. For continuous variables, normal distribution was evaluated with Kolmolgorov-Smirnov test, and logarithmic or square-root transformations were performed on continuous variables of nonnormal distribution. Differences among groups were analyzed by 1-way analysis of variance followed by post hoc analysis (Bonferroni correction). GLM univariate analysis of variance (2-way analysis of variance) followed by Tukey HSD and Bonferroni were applied for multiple comparisons when there were more than 2 factors influencing a variable (effect of time point and treatment options on cardiac function). All analyses used 2-sided tests with an overall significance level of α=0.05 and were performed with SPSS 15.0 for Mac.

Results

In Vitro Transduction: Localization and Confirmation

Depending on its subcellular location, intracellular S100A1 modulates cardiac Ca^{2+} turnover via different Ca^{2+}-regulatory proteins.[19] Our first goal was to demonstrate the location of endogenous S100A6 and that of our exogenous GFP-tagged S100A6 to ensure that binding to GFP (larger molecular mass of 27 kDa) did not change its localization and hence activity. Although transduced NRVMs showed predominantly cytoplasmic and perinuclear localization of exogenous GFP-tagged human S100A6 protein (Figure 1A), endogenous rat S100A6 showed predominantly cytoplasmic, but also nuclear localization (Figure 1B). We tested whether S100A6 could enter cells via endocytosis. After incubation of cells with exogenous S100A6-His fusion protein, staining for endogenous S100A6 and exogenous extracellular S100A6-His fusion protein showed the cytoplasmic uptake of exogenously added S100A6 in the presence of 2 mmol/L Ca^{2+} after 1 hour, which colocalized with endogenous S100A6 (both cytoplasmic and nuclear) (Figure 1C).

Real-time PCR data showed a significant rise in expression of human/rat S100A6 in S100A6-overexpressing cardiomyocytes and significantly decreased expression of endogenous rat S100A6 in S100A6 knockdown cardiomyocytes. Overexpression or knockdown of S100A6 had no influence on the expression of S100A1 or S100B (Figure 1D). We confirmed transduction of cardiomyocytes by Western blotting in S100A6-overexpressing and S100A6-knockdown cardiomyocytes, compared to null-plasmid transfected and nontransfected controls (Figure 1E).

Calcium Transients and CaN Activity In Vitro

Calcium transients of S100A6-knockdown and S100A6-overexpressing neonatal cardiomyocytes were quantified using the fluorophore (Fura-2AM) 2 days after viral transduction. S100A6-overexpressing neonatal cardiomyocytes showed significantly increased calcium release amplitude. Moreover, S100A6-knockdown cardiomyocytes showed transients that had significantly lower amplitude, and the overall Ca^{2+} release rate was significantly decreased in the S100A6-knockdown compared to control cardiomyocytes (Figure 2A and 2B).

CaN, a calcium-dependent serine-threonine phosphatase, has antiapoptotic effects on cardiomyocytes in vitro[20] and a cardioprotective role following myocardial I/R through the Nuclear factor of activated T-cells (NFAT) pathway.[21,22] The phosphatase activity of CaN is mostly dependent on the level of free calcium.[23] We measured the phosphatase activity of CaN in S100A6-overexpressing and S100A6-knockdown neonatal cardiomyocytes after H/R (24/6 hours) and normoxia compared to controls both as an indicator of free cytosolic calcium levels and as a key antiapoptotic molecule: CaN phosphatase activity was significantly higher in S100A6-overexpressing neonatal cardiomyocytes compared to null-transduced and nontransduced controls both after normoxia and H/R,(24/6 hours) (Figure 2C).

S100A6-overexpressing cardiomyocytes had significantly increased expression of CaN A after H/R compared to null-transduced and nontransduced controls, but S100A6 overexpression had no significant effect on CaN B, either during hypoxia or after H/R in vitro (Figure 2C).

Effect of S100A6 on Apoptosis After H/R In Vitro

We used H/R (1% O_2, 20% CO_2, and 79% N_2 at 37°C for 24 hours, followed by 95% air and 5% CO_2 at 37°C for 6 hours) as an in vitro surrogate for I/R. S100A6-overexpressing cardiomyocytes showed a significantly smaller number of apoptotic nuclei by TUNEL staining compared to null-transduced and nontransduced controls after H/R, whereas S100A6-knockdown cardiomyocytes showed a greater number of apoptotic nuclei both under normoxic conditions and after H/R (Figure 3A and 3B). TUNEL staining results were consistent with significantly lower caspase 3/7 activity in S100A6-overexpressing cardiomyocytes and higher caspase 3/7 activity in S100A6-knockdown cells compared to controls after H/R (Figure 3C).

Effect of S100A6 Gene Delivery via UTMD on Cardiac I/R Injury

We delivered human S100A6-N-emGFP plasmid DNA (500 μg of plasmid DNA [S100A6 or empty plasmid] coupled to 1×10^9

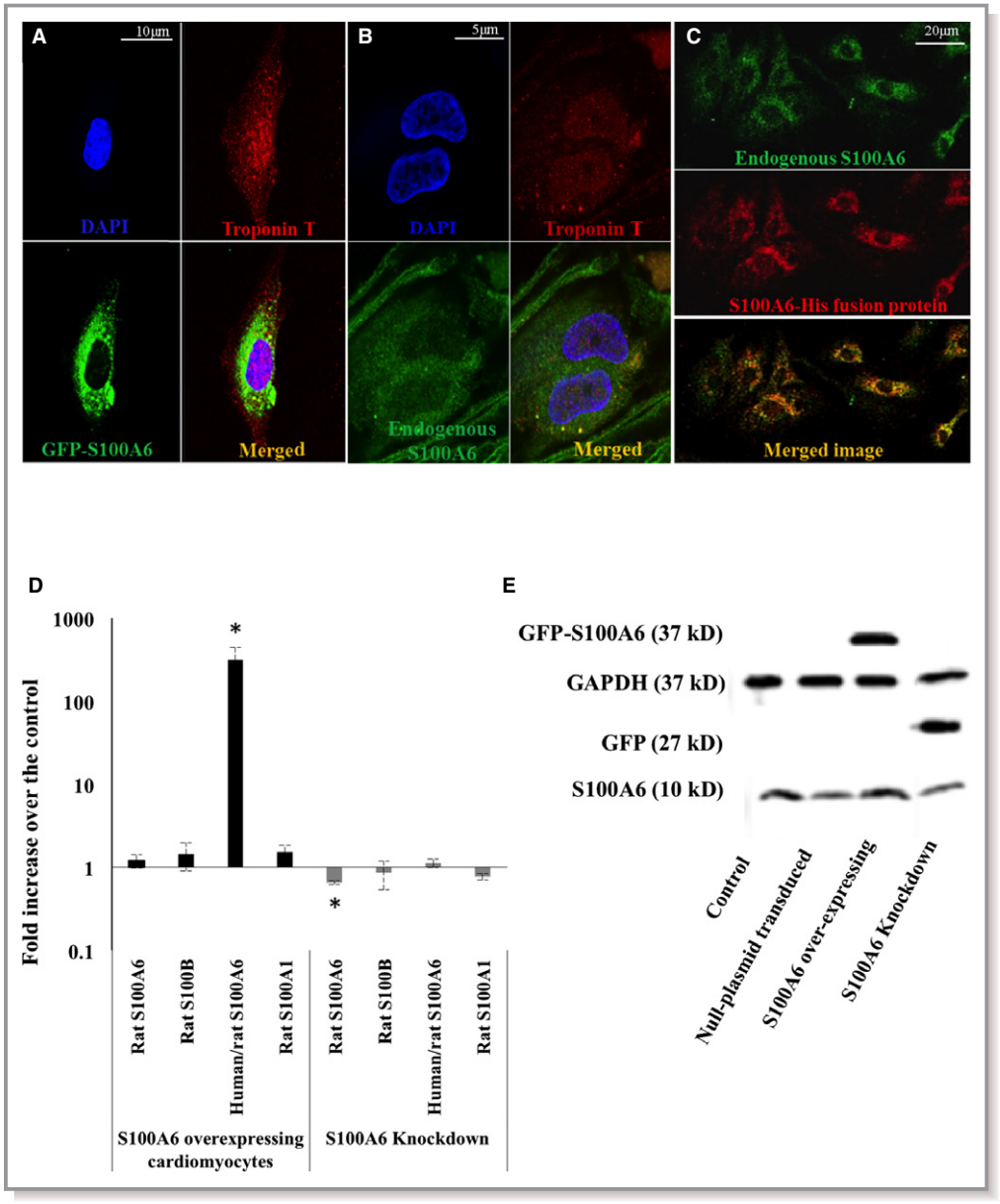

Figure 1. Localization and confirmation of in vitro transduction. Immunocytochemical staining of (A) exogenous GFP-tagged human S100A6 (green) in adenoviral-transduced neonatal cardiomyocytes showing perinuclear and cytoplasmic localization (magnification ×60) and (B) endogenous rat S100A6 (green) in neonatal cardiomyocytes showing cytoplasmic and nuclear localization (magnification ×60). C, Staining of endogenous S100A6 (top panel—green), S100A6-His fusion protein (middle panel—red) after cytoplasmic uptake of exogenously added S100A6 in the presence of 2 mmol/L Ca^{2+} after 1 hour, and colocalization (both cytoplasmic and nuclear) with endogenous S100A6 (bottom panel) (magnification ×20). D, Expression of rat-S100A6, rat-S100B, rat-S100A1 and exogenous human/rat-S100A6 mRNA in S100A6-overexpressing and S100A6-knockdown neonatal cardiomyocytes by qRT-PCR. Data expressed as mean±SEM, **P*<0.05 vs nontransduced controls, N=7 for each. Overexpression and downregulation of S100A6 did not affect the expression of S100A1 or S100B in vitro. E, Western blot in S100A6-overexpressing and S100A6-knockdown cardiomyocytes compared to null-plasmid– and nontransduced controls. DAPI, 4′,6-diamidino-2-phenylindole; GAPDH, glyceraldehyde 3-phosphate dehydrogenase; GFP, green fluorescent protein; qRT-PCR, quantitative real-time polymerase chain reaction.

cationic lipid microbubbles) by UTMD[18] 2 days prior to induction of I/R. UTMD of plasmid DNA results in peak transfection by day 2 to 3; thus, pretreatment allowed for maximal transgene expression at the time of cardiac I/R. The regional expression of S100A6 in the LV myocardium (anterior and posterior) on days 1, 7, and 28 post–cardiac I/R by

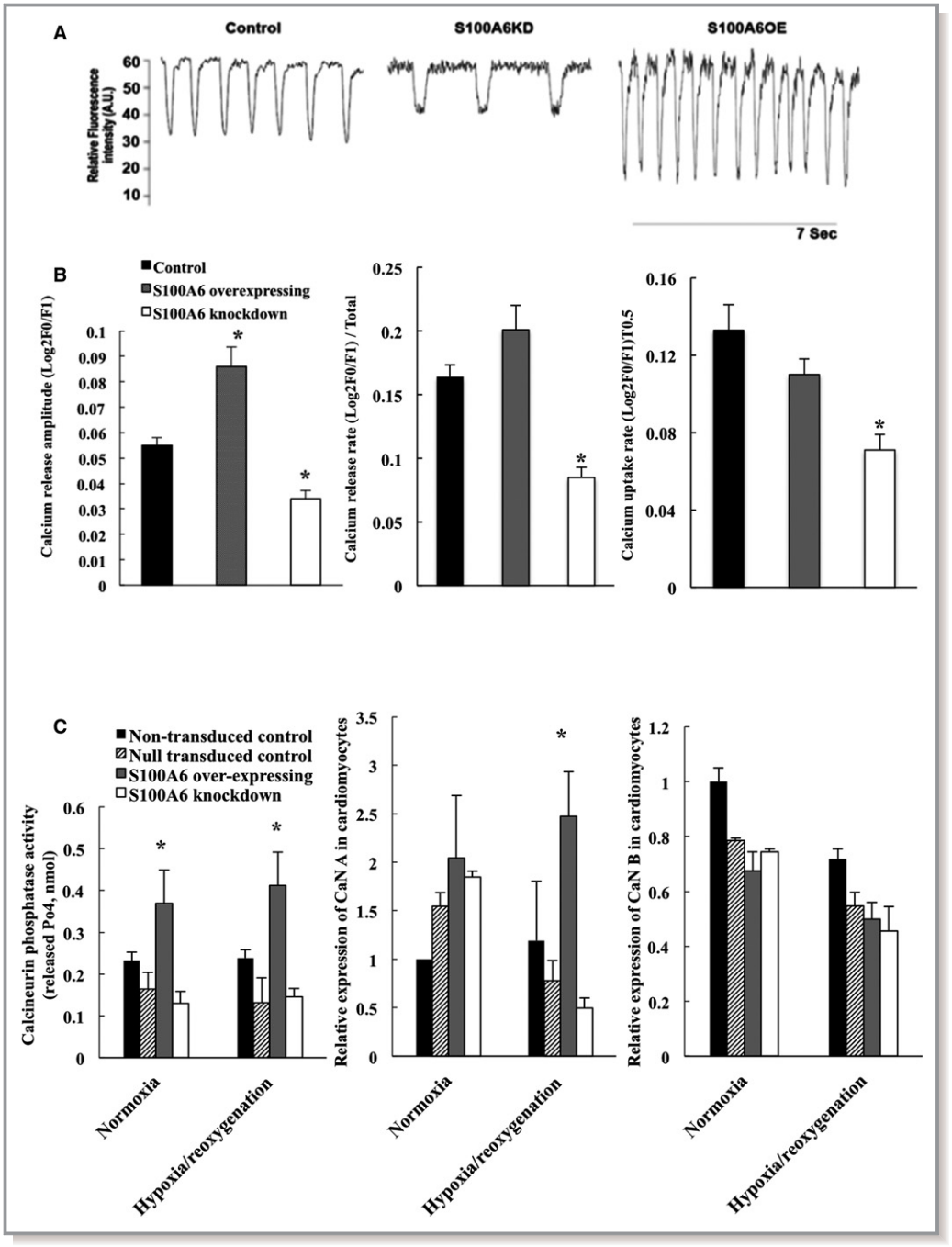

Figure 2. Calcium transients and calcineurin (CaN) activity in vitro. A, Representative calcium transient imaging for nontransduced control, S100A6-knockdown (KD) and S100A6-overexpressing (OE) cardiomyocytes. B, The calcium release amplitude, the rate of calcium release and uptake in S100A6-overexpressing and S100A6-knockdown neonatal cardiomyocytes compared to nontransduced controls during spontaneous action potentials (mean±SEM, **P*<0.05 vs nontransduced controls, N=7 for each). C, CaN phosphatase activity during normoxia and after H/R (24/6 hours) in S100A6-overexpressing and S100A6-knockdown neonatal cardiomyocytes compared to null-transduced and nontransduced controls and relative expression of CaN A and CaN B in S100A6-overexpressing, S100A6-knockdown, null-transduced, and nontransduced cardiomyocytes during normoxia and hypoxia/reoxygenation (mean±SEM, **P*<0.05 vs null-transduced and nontransduced controls, N=7 for each).

qRT-PCR (quantitative real-time PCR) is shown in Figure 4A through 4C. Our data show increased expression of human/rat S100A6 in the anterior LV of S100A6-treated rats at all time points post-I/R, with expression decreasing over time. S100A6 expression was lower in the posterior LV (Figure 4A through 4C).

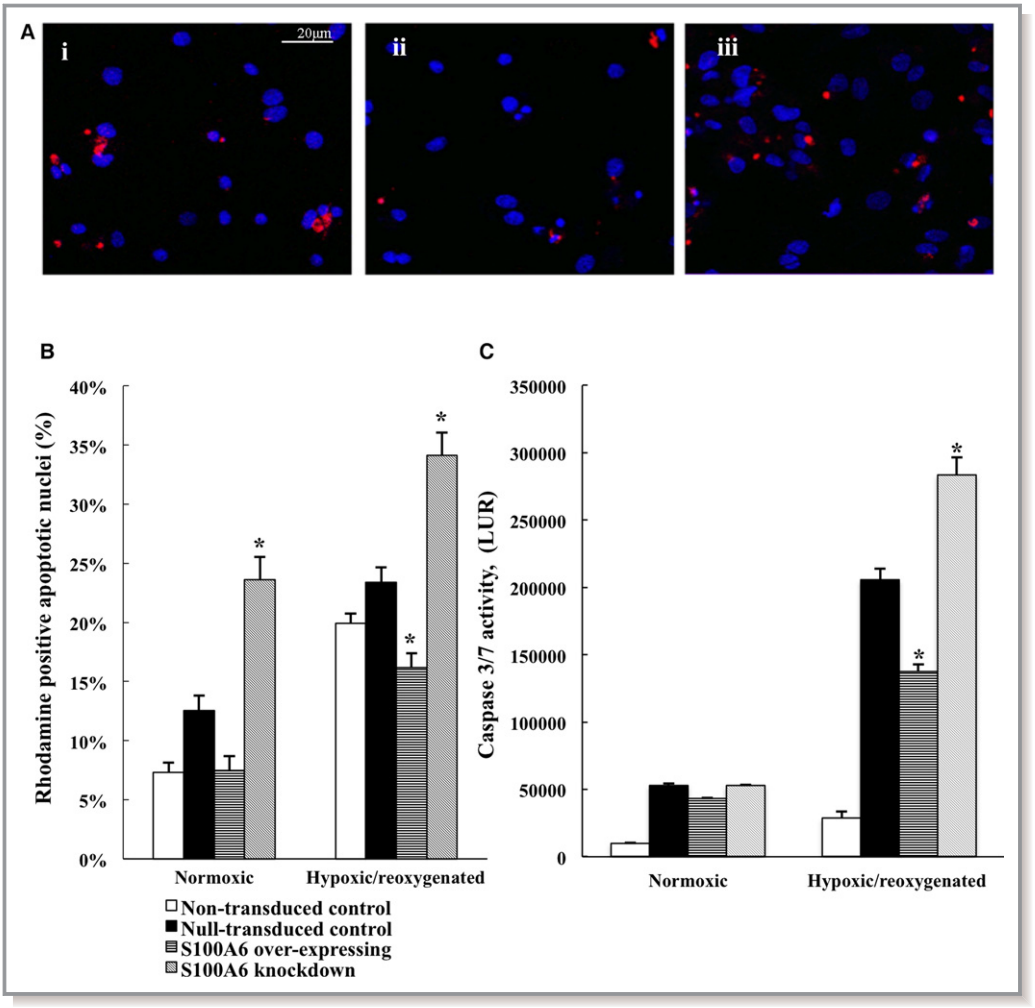

Figure 3. Effect of S100A6 on apoptosis after hypoxia/reoxygenation in vitro. S100A6 overexpression prevented hypoxia/reoxygenation (24/6 hours)-induced apoptosis in vitro, whereas S100A6-down-regulated cells showed greater apoptosis under normal conditions and after hypoxia/reoxygenation (24/6 hours). A, TUNEL staining in (i) nontransduced controls, (ii) S100A6-overexpressing, and (iii) S100A6-knockdown neonatal cardiomyocytes. Nuclei are stained by DAPI (blue) and apoptotic cells are rhodamine positive (red), ×60. B, Rhodamine-positive apoptotic neonatal cardiomyocytes detected by TUNEL staining in S100A6-overexpressing and S100A6-knockdown neonatal cardiomyocytes compared to null-transduced and nontransduced cells (mean±SEM, **P*<0.05 vs null-transduced controls, N=10 for each). C, Caspase 3/7 activity in S100A6-overexpressing and S100A6-knockdown neonatal cardiomyocytes compared to null-transduced and nontransduced control cells after hypoxia/reoxygenation (24/6 hours) (mean±SEM, **P*<0.05 vs null-transduced controls, N=10 for each). DAPI, 4′,6-diamidino-2-phenylindole; TUNEL, terminal deoxynucleotidyl transferase dUTP nick end labeling.

The mortality rate after I/R induction surgery was significantly lower in the S100A6-pretreated animals compared to empty-plasmid–treated and nontreated controls (25% versus 55% and 42%, respectively, $P<0.05$) (Figure 4D), with all mortality occurring during ischemia or immediately on reperfusion. The LV ejection fraction and fractional area change by 2D echocardiography progressively improved in the S100A6-treated group compared to empty-plasmid–treated and nontreated controls up to day 28. The circumferential extent of the akinetic segment of the LV progressively decreased in S100A6-treated rats from day 3 to day 28 and became significantly smaller than empty-plasmid–treated and nontreated controls (Figure 4E through 4H).

Effect of S100A6 Gene Delivery on Cardiac Hypertrophy and Fetal Gene Expression After Cardiac I/R Injury

Body weight changes over 28 days post–I/R induction surgery were not significantly different between groups (data not shown). At day 28, S100A6-treated animals had a significantly lower heart weight to tibia length and heart

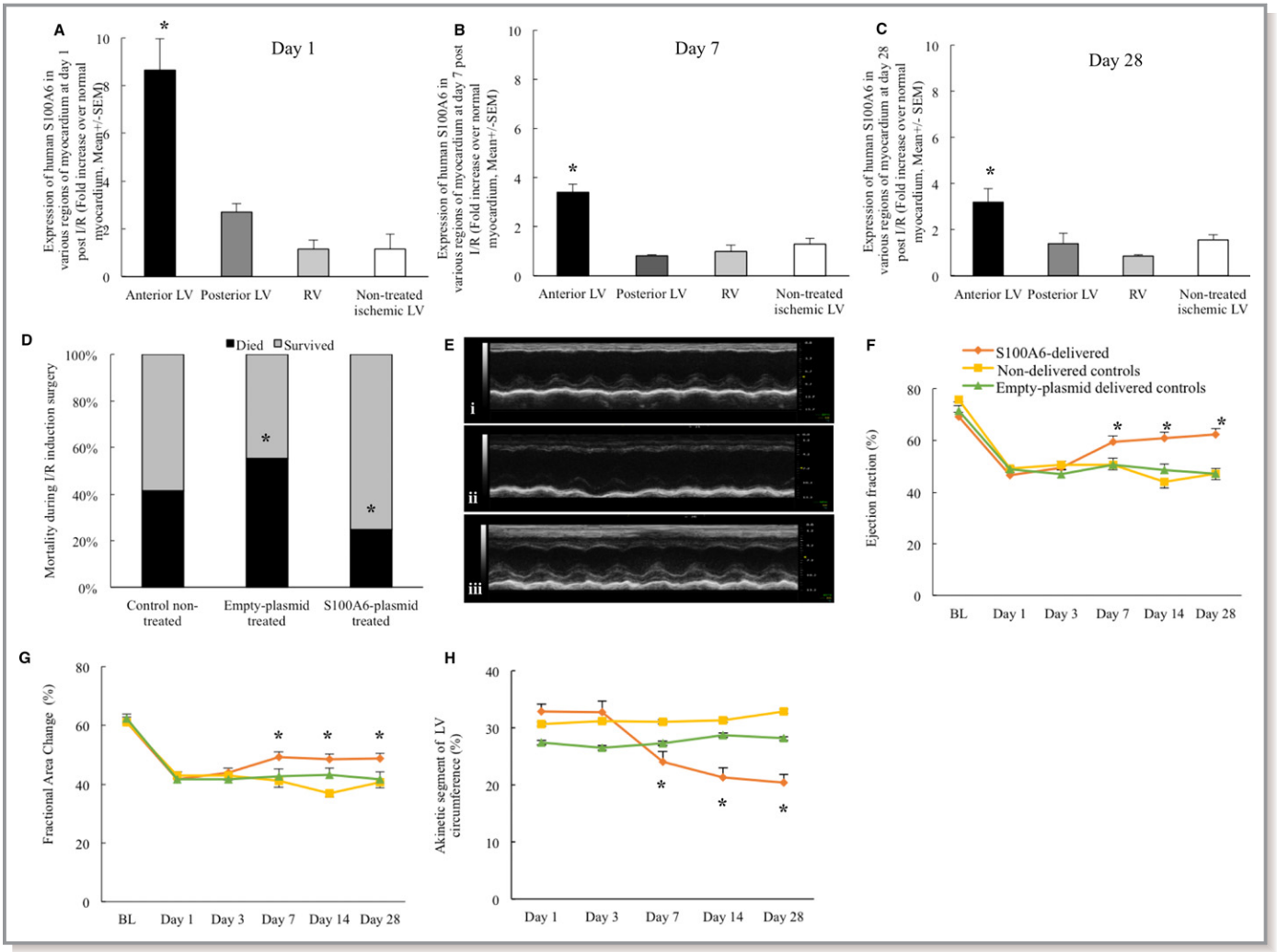

Figure 4. Effect of UTMD of S100A6 on myocardial ischemia-reperfusion. Exogenous human S100A6 gene expression by q RT-PCR in various regions of myocardium (anterior LV, posterior LV, and RV) at (A) day 1, (B) day 3, and (C) day 28 post–ischemia/reperfusion (I/R) normalized to normal nonischemic control myocardium (mean±SEM, **P*<0.05 vs all other groups, N=7 per group). D, Mortality rate during/after myocardial I/R in UTMD human-S100A6 plasmid-pretreated and UTMD empty-plasmid-pretreated rats compared to nontreated controls, N=29 per group. E, Representative M-mode echo image for (i) nontreated control, (ii) empty-plasmid-treated control, and (iii) UTMD S100A6-plasmid-treated. LV systolic function parameters ([F] ejection fraction and [G] fractional area change) following I/R in human-S100A6 plasmid-treated and empty plasmid-treated rats compared to nontreated controls (mean±SEM, **P*<0.05 vs nontreated and empty plasmid-treated controls, N=14-20 per group). H, Circumferential extent of LV akinesis following I/R in human-S100A6 plasmid-treated and empty plasmid-treated rats compared to nontreated control rats (mean±SEM, **P*<0.05 vs non-treated and empty plasmid-treated controls, N=14-20 per group). LV, left ventricle; RV, right ventricle; qRT-PCR, quantitative real-time polymerase chain reaction; UTMD, ultrasound-targeted microbubble destruction.

weight to body weight ratios compared to empty-plasmid–treated and nontreated controls (Figure 5A and 5B). In keeping with less cardiac hypertrophy in S100A6-treated hearts, cardiomyocyte size was significantly smaller in S100A6-treated rats in comparison to empty-plasmid– and nontreated controls at day 28 following I/R (Figure 5D). S100A6-treated hearts had significantly lower expression of βMHC and ANF, markers of myocardial hypertrophic phenotype, in the infarct and noninfarct regions of myocardium 28 days after I/R compared to empty-plasmid–treated and nontreated controls (Figure 5E and 5F).

Effect of S100A6 Gene Delivery on Infarct Size and Myocardial Viability (Necrosis and Apoptosis)

Despite pretreatment with S100A6 gene therapy 2 days before I/R, the risk area by Evans blue was similar across all treatment groups (Figure 6A and 6C). We used TTC staining to mark the infarcted area in LV myocardial sections 24 hours post-I/R, demonstrating that S100A6-treated rats had significantly smaller infarct size/nonviable myocardium at 24 hours post-I/R (control 24.8%, empty-treated 25.6%, and S100A6-treated 14.7%) (Figure 6B and 6E). Using Masson trichrome staining on LV sections at day 28 post-I/R, we

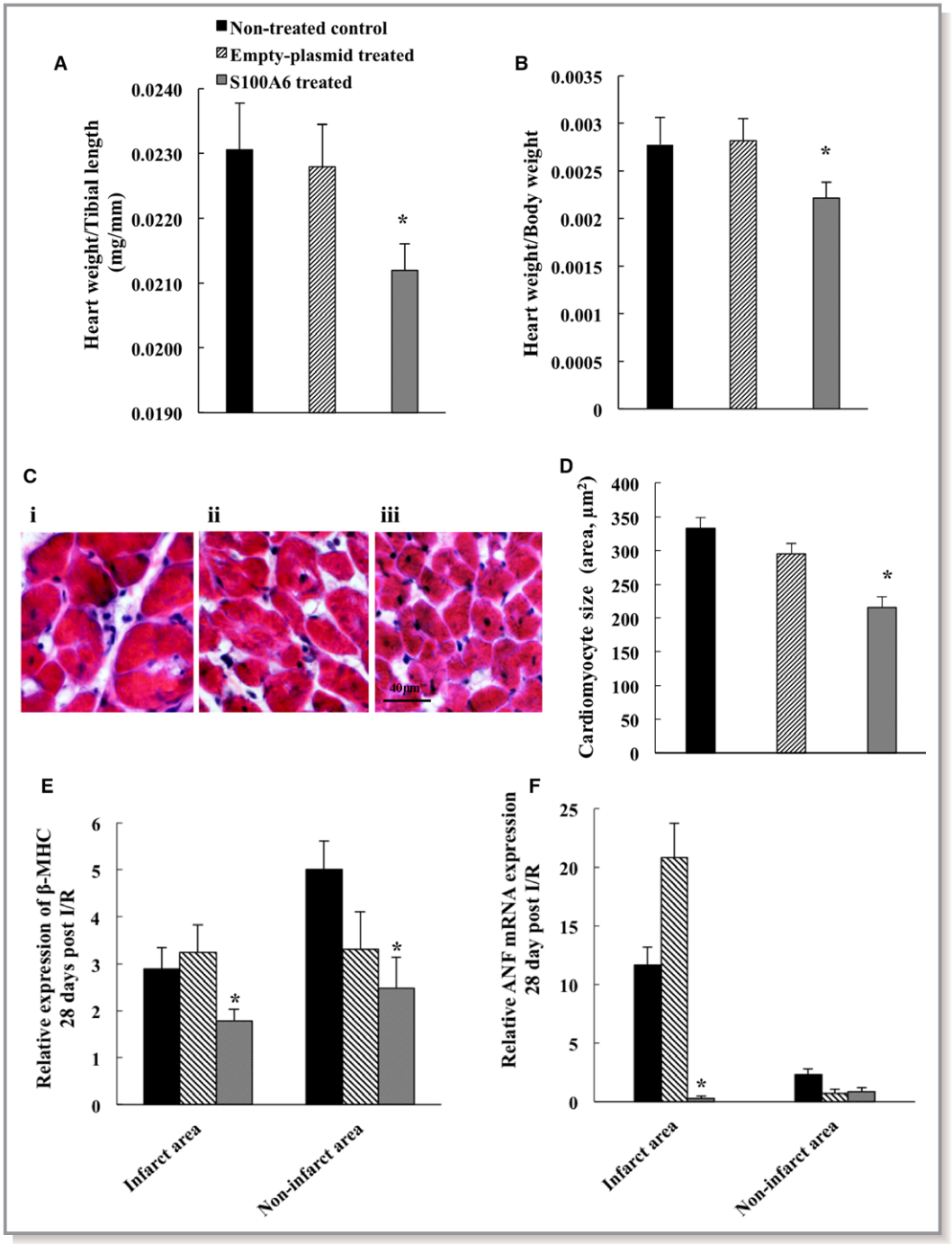

Figure 5. Cardiac hypertrophy data post–myocardial ischemia-reperfusion. A, Ratio of heart weight to tibia length at day 28 post-I/R (mean±SEM, **P*<0.05 vs nontreated and empty plasmid–treated controls, N=14-20 in each group). B, Ratio of heart weight to body weight at day 28 post-I/R (mean±SEM, **P*<0.05 vs nontreated and empty plasmid–treated controls, N=14-20 in each group). C, Representative H&E-stained images of noninfarct sections of LV myocardium at day 28 post-I/R in (i) control, (ii) empty plasmid, and (iii) S100A6 plasmid delivered rats. D, Cardiomyocyte size at day 28 post-I/R (magnification ×100) (mean±SEM, **P*<0.05 vs nontreated and empty plasmid–treated controls, N=50-60 cells in each group). E, Relative expression of βMHC in the infarct and noninfarct regions of myocardium 28 days post-I/R (mean±SEM, **P*<0.05 vs nontreated and empty plasmid–treated controls, N=7 for all groups). F, Relative expression of ANF in the infarct and noninfarct regions of myocardium 28 days post-I/R (mean±SEM, **P*<0.05 vs nontreated and empty plasmid–treated controls, N=7 for all groups). ANF, atrial natriuretic factor; βMHC, β-myosin heavy chain; H&E, hematoxylin and eosin; I/R, ischemia-reperfusion.

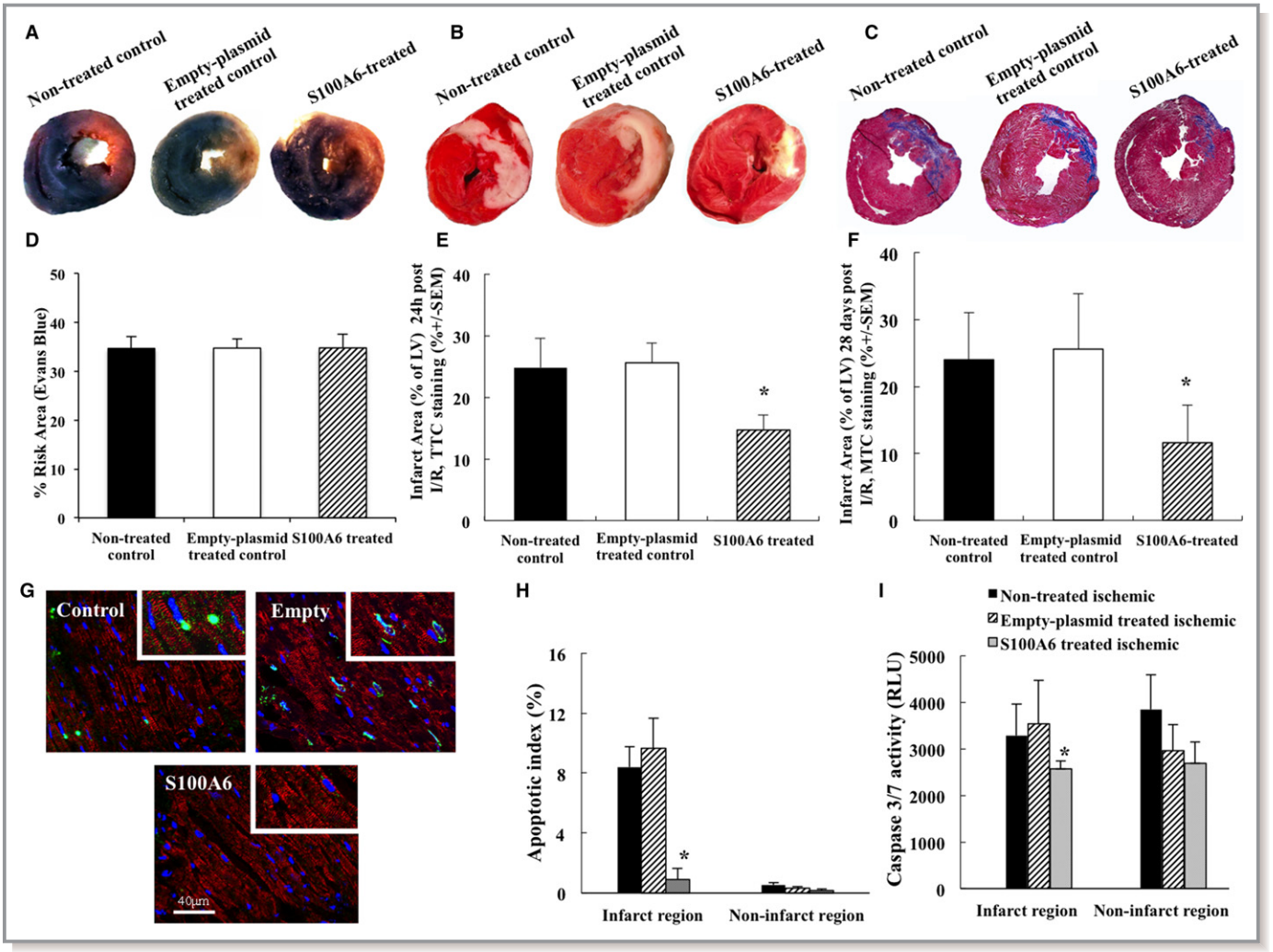

Figure 6. Infarct size and apoptosis data post–myocardial ischemia-reperfusion. A, Representative Evans blue–stained myocardial sections during ligation of the left anterior descending coronary artery, outlining the area at risk in nontreated controls, empty plasmid–treated controls, and human-S100A6 plasmid–treated rats. B, Representative TTC-stained myocardial cryosections 1 day post-I/R in nontreated controls, empty plasmid–treated controls, and human-S100A6 plasmid–treated rats. The nonviable/infarcted myocardium is white, and viable myocardium is red/pink. C, Representative MTC-stained myocardial cryosections 28 days post-I/R in nontreated controls, empty plasmid–treated controls, and human-S100A6 plasmid–treated rats. The collagen debris in the central compact necrotic region of the infarcted area is shown in blue, myocardial fibers in pink, and nuclei in purple. D, Risk area by Evans blue as percentage of the LV (mean±SEM, N=6 per group). E, Nonviable myocardium/infarct area by TTC staining as percentage of the LV (mean±SEM, **P*<0.05 vs nontreated and empty plasmid–treated controls, N=9 per group). F, Infarct area/scar size by MTC staining as a percentage of the LV (mean±SEM, **P*<0.05 vs nontreated and empty plasmid–treated controls, N=8-9 per group). G, IHC staining of infarct region of myocardium 1 day post-I/R (sarcomeric α-actinin [red], nuclei [blue], and fluorescein isothiocyanate [FITC]-positive apoptotic nuclei [green]) (magnification ×40). H, Data on apoptotic index in infarct and noninfarct regions in myocardial cryosections 1 day post-I/R in human-S100A6 plasmid–treated and empty plasmid–treated rats compared to nontreated controls (mean±SEM, **P*<0.05 vs nontreated and empty-treated controls, N=7-9 for each group). I, Caspase 3/7 activity in the infarct and noninfarct regions of myocardium 1 day post-I/R in S100A6-treated and empty plasmid–treated rats compared to nontreated controls (mean±SEM, **P*<0.05 vs nontreated and empty-treated controls, N=6 in each group). LV, left ventricle; MTC, Masson trichrome; TTC, 2,3,5-triphenyl-tetrazolium chloride.

showed significantly smaller collagen-rich scar tissue in the LV of S100A6-treated rats compared to nontreated and empty-treated controls (control 24.0%, empty-treated 25.6%, and S100A6-treated 11.6%) (Figure 6C and 6F). These data show that S100A6 overexpression reduces acute infarct size and leads to a greater extent of viable myocardium post-I/R, smaller infarct scar size, thus allowing improved late recovery of LV systolic function.

We examined the antiapoptotic effects of S100A6 pretreatment in the myocardium at day 1 after I/R by TUNEL and caspase 3/7 activity assay. S100A6-pretreated animals showed significantly lower numbers of apoptotic cells by

TUNEL staining in the infarct and noninfarct regions of myocardium compared to empty-plasmid– and nontreated controls 28 days after I/R (Figure 6E and 6F). Caspase 3/7 activity at day 1 post-I/R was lower in the infarcted myocardium of S100A6-pretreated animals compared to empty-plasmid– and nontreated controls (Figure 6G). This finding is consistent with our in vitro data on S100A6-overexpressing neonatal cardiomyocytes post-H/R and suggests that the prosurvival effect of S100A6 during myocardial I/R injury is in part through inhibition of the intrinsic pathway of apoptosis. The magnitude of difference between S100A6-treated hearts and controls is greater for TUNEL (5- to 6-fold decrease) as compared to caspase activity (<2-fold). This may reflect the detection of myocytes in the early stages of necrosis rather than apoptosis by TUNEL as well as detection of caspase-independent pathways of apoptosis.[24]

Discussion

Cardiac I/R injury after coronary reperfusion is a complex biologic process involving a wide range of pathological processes at the cellular and molecular levels, and although many therapeutic strategies have shown benefit in experimental studies, their impact on current clinical practice has been modest.[9,11] Ours is the first study of S100A6 gene therapy for myocardial I/R, demonstrating that S100A6, an EF-hand Ca^{2+}-binding protein, is able to impact several pathways involved in acute I/R, leading to increased survival, smaller infarct size, and improved LV systolic function 4 weeks after acute myocardial infarction.

S100A6 is a low-molecular-weight calcium-binding protein belonging to the S100 family consisting of about 24 small dimeric (~20 kDa) EF calcium-binding proteins implicated in various intracellular and extracellular activities.[25] The genes encoding at least 16 of the S100 proteins, including S100A6, are primarily located in a cluster on chromosome 1 in humans and are denoted S100A1 to S100A16. S100 proteins that fall outside of this gene locus are given single-letter names (ie, S100B to chromosome 21).[26] The S100A6 gene encodes a polypeptide of 89 amino acids that has 55 (52%) identical residues with S100B (90 amino acid residues) and S100A1 (94 amino acid residues), respectively.[27] In spite of significant sequence similarities, the S100 proteins fulfill nonredundant roles and reveal different expression patterns.[25] In cells, S100 proteins are present mainly in the cytoplasm and exist in the form of noncovalent dimers. Each S100 monomer is able to bind calcium via the EF-hand motifs, inducing a conformational change and allowing interaction with diverse target proteins. An S100 monomer has 2 helix-loop-helix EF-hand calcium-binding domains connected by a linker region termed the hinge region. The EF-hand in the N-terminal region of the protein is 14 amino acids in length and called the pseudo-EF-hand and binds calcium mostly through main-chain carbonyl groups, resulting in a weak calcium affinity with K_ds ~200 to 500 μmol/L (ie, S100B K_d>350 μmol/L). The second EF-hand is a canonical 12-residue C-terminal EF-hand that ligates calcium in a similar manner to calmodulin and troponin C, resulting in a higher-calcium-affinity site with K_ds ~1 to 50 μmol/L (ie, S100A6 K_d≈3 μmol/L, S100A1 K_d≈27 μmol/L, and S100B K_d≈50 μmol/L).[25] The S100A6 target proteins identified thus far include mostly cytoskeletal proteins and components of heat shock protein complexes.[28] It has been demonstrated that the calcium-dependent binding of S100A6 to its targets could interfere with their phosphorylation or could disrupt protein-protein interactions through competition.[29] The role of extracellular S100A6 is not clear at present, but the obtained results suggest a possible involvement in cell survival through its binding to the transmembrane receptor for advanced glycation endproducts.[30]

Comparisons between S100A6 and S100A1, the most widely studied members of the S100 family of EF-hand calcium-binding proteins, show key similarities but also demonstrate important differences. Whereas S100A1 is highly expressed under basal conditions and is downregulated post-MI,[31] S100A6 exhibits low basal cardiac expression with upregulation after acute MI.[14] Forced expression of S100A6 in cardiomyocytes prevented apoptosis by interfering with p53 phosphorylation[15] and inhibited the induction of the cardiac fetal gene promoters β-myosin heavy chain and skeletal α-actin.[14] Cardiomyocyte-specific transgenic mice overexpressing S100A6 subjected to permanent LAD coronary ligation had less myocyte hypertrophy, interstitial fibrosis, and cardiomyocyte apoptosis, leading to greater preservation of LV systolic function compared to control animals.

The results of our study add to the existing data on S100A6, showing that S100A6 gene therapy delivered 2 days prior to LAD ligation and reperfusion helped ameliorate cardiac I/R injury. We performed LAD ligation and reperfusion blinded to which pretreatment animals had received, thereby allowing us to use mortality as 1 of the endpoints. Although S100A6 gene therapy provided a survival advantage after I/R, the challenge for translating this to clinical practice will be optimizing gene delivery for rapid transfection prior to or immediately after reperfusion. The exact mechanism behind this protective effect is unclear; however, we can speculate that the enhanced Ca^{2+} cycling would attenuate diastolic Ca^{2+} overload, thus suppressing arrhythmogenesis and leading to a reduction in reperfusion arrhythmias.[32,33] All mortality occurred during occlusion or immediately on reperfusion, supporting an arrhythmic death.

We examined the role of intracellular S100A6 on Ca^{2+} homeostasis in neonatal ventricular cardiomyocytes in vitro. Whereas overexpression of S100A6 lead to increased amplitude of Ca^{2+} transients with enhanced release and uptake rates

between the sarcoplasmic reticulum and the cytosol, knockdown of S100A6 had the opposite results. Our findings are in contrast to the results of Wang et al, who found that S100A6 did not significantly alter Ca^{2+} transients.[34] Our study used rhythmically beating neonatal cardiac myocytes during spontaneous action potentials, whereas they investigated the effect of S100A6 calcium handling in nonbeating adult cardiomyocytes during stimulated action potentials. Adult cardiomyocytes undergo phenotypic changes after isolation and culture and lack spontaneous contraction. These distinctions over neonatal cardiomyocytes and variations in calcium handling between stimulated action potentials and spontaneous depolarization likely account for the differences between studies.[35,36] We believe that the contractile profile during H/R of cultured neonatal myocytes is more compatible with in situ hearts during I/R. This effect on intracellular calcium transients is similar to that of S100A1,[19,37] where intracellular S100A1 overexpression enhanced the Ca^{2+}-transient amplitude in cardiomyocytes via a stimulatory action on sarco/endoplasmic reticulum Ca^{2+}-ATPase and ryanodine receptor 2. Our data on enhanced Ca^{2+} transients is the likely link to increased CaN activity, which is driven by higher availability of free Ca^{2+}.[23] Given the prosurvival and antiapoptotic role of CaN-NFAT signaling in the heart,[20-22] the enhanced CaN activity likely contributed to the existing antiapoptotic effects of S100A6 mediated through p53 phosphorylation.[15] In contrast to S100A6 effects, extracellular S100A1 inhibits apoptosis in cardiomyocytes via activation of extracellular signal-regulated kinase 1/2.[38] Although intracellular S100A1 also binds to p53,[39] whether this plays a role in the antiapoptotic effect of S100A1 has not been examined. To our knowledge, S100A1 effects on CaN have not been studied. Indeed, S100A1-provoked Ca^{2+} cycling appears to bypass Ca^{2+}-dependent hypertrophic pathways such as those that involve activation of protein kinase C and CaN.[40]

Recently, the role of S100A6 in endothelial cell proliferation has been elucidated.[41] Lerchenmuller et al reported a previously unrecognized link between S100A6 and attenuation of the antiproliferative signal transducers and activators of transcription 1 (STAT1) in endothelial cells. In their study, S100A6-depleted endothelial cells had activated STAT1, whereas knockdown of STAT1 restored their proliferative capacity via suppression of its downstream effector interferon-inducible transmembrane protein 1.[41] Given that STAT1 activation plays a role in I/R-induced apoptosis,[42] and STAT1 deficiency protects against myocardial infarction injury by enhancing autophagy,[43] whether the positive effects of S100A6 on myocardial I/R are in part mediated by modulation of STAT1 signaling in cardiomyocytes is worthy of future study.

There are several important limitations to our study. The main limitation is that S100A6 gene therapy was delivered 2 days prior to coronary ligation. We did this to ensure maximal transfection at the time of I/R, given that peak transfection of 3 days with UTMD[44] would prove less beneficial in the context of the rapid response to injury. Our results still provide important proof-of-concept data on the therapeutic benefit of S1006 therapy for prevention of cardiac I/R injury. We fully understand that for clinical translation, more efficient, rapid transfection techniques will be required for gene therapy at the time of reperfusion, or protein-based therapies will need to be considered. Our recent work on UTMD of miRNA[45] showing transfection as early as 3 hours post-UTMD suggests that miRNAs could be an effective gene strategy to combat myocardial infarction and I/R injury.[46] Finally, Ca^{2+} transients were measured during the absence of stress. Further studies examining Ca^{2+} transients under stimulation and after H/R are warranted.

In summary, the present study is the first to demonstrate the therapeutic benefit of S100A6 gene therapy, with improved survival, reduced infarct size, and greater myocardial viability resulting in increased LV systolic function in the setting of acute MI and I/R injury. These positive effects were attributable not only to the known antiapoptotic and antihypertrophic effects of S100A6 but also to enhanced Ca^{2+} cycling and CaN phosphatase activity. These results warrant further studies exploring the therapeutic potential of S100A6 in cardiac diseases.

Sources of Funding

This work is supported by Operating Grants (MOP 62763 and MOP 137109) from the Canadian Institutes of Health Research, Ottawa, Ontario, Canada, and an Infrastructure Grant from the Canadian Foundation for Innovation (26222), Ottawa, Ontario, Canada. Dr Leong-Poi holds the Brazilian Ball Chair in Cardiology from St. Michael's Hospital, University of Toronto, Canada. Dr Gramolini holds a Canada Research Chair in Cardiovascular Proteomics and Molecular Therapeutics from the University Health Network, University of Toronto, Canada. Dr Connelly holds a New Investigator Award from the Canadian Institutes of Health Research, Ottawa, Ontario, Canada.

Disclosures

None.

References

1. Armstrong PW, Gershlick AH, Goldstein P, Wilcox R, Danays T, Lambert Y, Sulimov V, Rosell Ortiz F, Ostojic M, Welsh RC, Carvalho AC, Nanas J, Arntz HR, Halvorsen S, Huber K, Grajek S, Fresco C, Bluhmki E, Regelin A, Vandenberghe K, Bogaerts K, Van de Werf F. Fibrinolysis or primary PCI in ST-segment elevation myocardial infarction. *N Engl J Med*. 2013;368:1379–1387.
2. Bainey KR, Ferguson C, Ibrahim QI, Tyrrell B, Welsh RC. Impact of reperfusion strategy on aborted myocardial infarction: insights from a large Canadian ST-Elevation Myocardial Infarction Clinical Registry. *Can J Cardiol*. 2014;30:1570–1575.
3. Sugiyama T, Hasegawa K, Kobayashi Y, Takahashi O, Fukui T, Tsugawa Y. Differential time trends of outcomes and costs of care for acute myocardial infarction hospitalizations by ST elevation and type of intervention in the

United States, 2001–2011. *J Am Heart Assoc*. 2015;4:e001445. DOI: 10.1161/JAHA.114.001445.

4. Lambert LJ, Brophy JM, Racine N, Rinfret S, L'Allier PL, Brown KA, Boothroyd LJ, Ross D, Segal E, Kouz S, Maire S, Harvey R, Kezouh A, Nasmith J, Bogaty P. Outcomes of patients with ST-elevation myocardial infarction receiving and not receiving reperfusion therapy: the importance of examining all patients. *Can J Cardiol*. 2016;32:1325.e1311–1325.e1318.
5. Giustino G, Baber U, Stefanini GG, Aquino M, Stone GW, Sartori S, Steg PG, Wijns W, Smits PC, Jeger RV, Leon MB, Windecker S, Serruys PW, Morice MC, Camenzind E, Weisz G, Kandzari D, Dangas GD, Mastoris I, Von Birgelen C, Galatius S, Kimura T, Mikhail G, Itchhaporia D, Mehta L, Ortega R, Kim HS, Valgimigli M, Kastrati A, Chieffo A, Mehran R. Impact of clinical presentation (stable angina pectoris vs unstable angina pectoris or non-ST-elevation myocardial infarction vs ST-elevation myocardial infarction) on long-term outcomes in women undergoing percutaneous coronary intervention with drug-eluting stents. *Am J Cardiol*. 2015;116:845–852.
6. Chen HY, Tisminetzky M, Lapane KL, Yarzebski J, Person SD, Kiefe CI, Gore JM, Goldberg RJ. Decade-long trends in 30-day rehospitalization rates after acute myocardial infarction. *J Am Heart Assoc*. 2015;4:e002291. DOI: 10.1161/JAHA.115.002291.
7. Yellon DM, Hausenloy DJ. Myocardial reperfusion injury. *N Engl J Med*. 2007;357:1121–1135.
8. Eltzschig HK, Eckle T. Ischemia and reperfusion—from mechanism to translation. *Nat Med*. 2011;17:1391–1401.
9. Hausenloy DJ, Yellon DM. Myocardial ischemia-reperfusion injury: a neglected therapeutic target. *J Clin Invest*. 2013;123:92–100.
10. Hausenloy DJ, Erik Botker H, Condorelli G, Ferdinandy P, Garcia-Dorado D, Heusch G, Lecour S, van Laake LW, Madonna R, Ruiz-Meana M, Schulz R, Sluijter JP, Yellon DM, Ovize M. Translating cardioprotection for patient benefit: position paper from the working group of cellular biology of the heart of the European Society of Cardiology. *Cardiovasc Res*. 2013;98:7–27.
11. Kloner RA. Current state of clinical translation of cardioprotective agents for acute myocardial infarction. *Circ Res*. 2013;113:451–463.
12. Nowotny M, Bhattacharya S, Filipek A, Krezel AM, Chazin W, Kuznicki J. Characterization of the interaction of calcyclin (S100A6) and calcyclin-binding protein. *J Biol Chem*. 2000;275:31178–31182.
13. Cai XY, Lu L, Wang YN, Jin C, Zhang RY, Zhang Q, Chen QJ, Shen WF. Association of increased S100B, S100A6 and S100P in serum levels with acute coronary syndrome and also with the severity of myocardial infarction in cardiac tissue of rat models with ischemia-reperfusion injury. *Atherosclerosis*. 2011;217:536–542.
14. Tsoporis JN, Marks A, Haddad A, O'Hanlon D, Jolly S, Parker TG. S100A6 is a negative regulator of the induction of cardiac genes by trophic stimuli in cultured rat myocytes. *Exp Cell Res*. 2005;303:471–481.
15. Tsoporis JN, Izhar S, Parker TG. Expression of S100A6 in cardiac myocytes limits apoptosis induced by tumor necrosis factor-α. *J Biol Chem*. 2008;283:30174–30183.
16. Tsoporis JT, Izhar S, Desjardins JF, Leong-Poi H, Parker TG. Conditional cardiac overexpression of S100A6 attenuates myocyte hypertrophy and apoptosis following myocardial infarction. *Curr Pharm Des*. 2014;20:1941–1949.
17. Bousette N, Abbasi C, Chis R, Gramolini AO. Calnexin silencing in mouse neonatal cardiomyocytes induces Ca^{2+} cycling defects, ER stress, and apoptosis. *J Cell Physiol*. 2014;229:374–383.
18. Lee PJ, Rudenko D, Kuliszewski MA, Liao C, Kabir MG, Connelly KA, Leong-Poi H. Survivin gene therapy attenuates left ventricular systolic dysfunction in doxorubicin cardiomyopathy by reducing apoptosis and fibrosis. *Cardiovasc Res*. 2014;101:423–433.
19. Most P, Boerries M, Eicher C, Schweda C, Volkers M, Wedel T, Sollner S, Katus HA, Remppis A, Aebi U, Koch WJ, Schoenenberger CA. Distinct subcellular location of the Ca^{2+}-binding protein S100A1 differentially modulates Ca^{2+}-cycling in ventricular rat cardiomyocytes. *J Cell Sci*. 2005;118:421–431.
20. De Windt LJ, Lim HW, Taigen T, Wencker D, Condorelli G, Dorn GW II, Kitsis RN, Molkentin JD. Calcineurin-mediated hypertrophy protects cardiomyocytes from apoptosis in vitro and in vivo: an apoptosis-independent model of dilated heart failure. *Circ Res*. 2000;86:255–263.
21. Obasanjo-Blackshire K, Mesquita R, Jabr RI, Molkentin JD, Hart SL, Marber MS, Xia Y, Heads RJ. Calcineurin regulates NFAT-dependent iNOS expression and protection of cardiomyocytes: co-operation with Src tyrosine kinase. *Cardiovasc Res*. 2006;71:672–683.
22. Bueno OF, Lips DJ, Kaiser RA, Wilkins BJ, Dai YS, Glascock BJ, Klevitsky R, Hewett TE, Kimball TR, Aronow BJ, Doevendans PA, Molkentin JD. Calcineurin Aβ gene targeting predisposes the myocardium to acute ischemia-induced apoptosis and dysfunction. *Circ Res*. 2004;94:91–99.
23. Perrino BA, Ng LY, Soderling TR. Calcium regulation of calcineurin phosphatase activity by its B subunit and calmodulin. Role of the autoinhibitory domain. *J Biol Chem*. 1995;270:340–346.
24. Cande C, Cecconi F, Dessen P, Kroemer G. Apoptosis-inducing factor (AIF): key to the conserved caspase-independent pathways of cell death? *J Cell Sci*. 2002;115:4727–4734.
25. Donato R, Cannon BR, Sorci G, Riuzzi F, Hsu K, Weber DJ, Geczy CL. Functions of S100 proteins. *Curr Mol Med*. 2013;13:24–57.
26. Ridinger K, Ilg EC, Niggli FK, Heizmann CW, Schafer BW. Clustered organization of S100 genes in human and mouse. *Biochim Biophys Acta*. 1998;1448:254–263.
27. Filipek A, Michowski W, Kuznicki J. Involvement of S100A6 (calcyclin) and its binding partners in intracellular signaling pathways. *Adv Enzyme Regul*. 2008;48:225–239.
28. Lesniak W, Slomnicki LP, Filipek A. S100A6—new facts and features. *Biochem Biophys Res Commun*. 2009;390:1087–1092.
29. Spiechowicz M, Zylicz A, Bieganowski P, Kuznicki J, Filipek A. Hsp70 is a new target of Sgt1—an interaction modulated by S100A6. *Biochem Biophys Res Commun*. 2007;357:1148–1153.
30. Leclerc E, Fritz G, Weibel M, Heizmann CW, Galichet A. S100B and S100A6 differentially modulate cell survival by interacting with distinct RAGE (receptor for advanced glycation end products) immunoglobulin domains. *J Biol Chem*. 2007;282:31317–31331.
31. Tsoporis JN, Marks A, Zimmer DB, McMahon C, Parker TG. The myocardial protein S100A1 plays a role in the maintenance of normal gene expression in the adult heart. *Mol Cell Biochem*. 2003;242:27–33.
32. Wang S, Chen J, Valderrabano M. Nutrient restriction preserves calcium cycling and mitochondrial function in cardiac myocytes during ischemia and reperfusion. *Cell Calcium*. 2012;51:445–451.
33. del Monte F, Lebeche D, Guerrero JL, Tsuji T, Doye AA, Gwathmey JK, Hajjar RJ. Abrogation of ventricular arrhythmias in a model of ischemia and reperfusion by targeting myocardial calcium cycling. *Proc Natl Acad Sci USA*. 2004;101:5622–5627.
34. Wang W, Asp ML, Guerrero-Serna G, Metzger JM. Differential effects of S100 proteins A2 and A6 on cardiac Ca(2+) cycling and contractile performance. *J Mol Cell Cardiol*. 2014;72:117–125.
35. Poindexter BJ, Smith JR, Buja LM, Bick RJ. Calcium signaling mechanisms in dedifferentiated cardiac myocytes: comparison with neonatal and adult cardiomyocytes. *Cell Calcium*. 2001;30:373–382.
36. Seki S, Nagashima M, Yamada Y, Tsutsuura M, Kobayashi T, Namiki A, Tohse N. Fetal and postnatal development of Ca^{2+} transients and Ca^{2+} sparks in rat cardiomyocytes. *Cardiovasc Res*. 2003;58:535–548.
37. Kettlewell S, Most P, Currie S, Koch WJ, Smith GL. S100A1 increases the gain of excitation-contraction coupling in isolated rabbit ventricular cardiomyocytes. *J Mol Cell Cardiol*. 2005;39:900–910.
38. Most P, Boerries M, Eicher C, Schweda C, Ehlermann P, Pleger ST, Loeffler E, Koch WJ, Katus HA, Schoenenberger CA, Remppis A. Extracellular S100A1 protein inhibits apoptosis in ventricular cardiomyocytes via activation of the extracellular signal-regulated protein kinase 1/2 (ERK1/2). *J Biol Chem*. 2003;278:48404–48412.
39. Fernandez-Fernandez MR, Rutherford TJ, Fersht AR. Members of the S100 family bind p53 in two distinct ways. *Protein Sci*. 2008;17:1663–1670.
40. Most P, Remppis A, Pleger ST, Katus HA, Koch WJ. S100A1: a novel inotropic regulator of cardiac performance. Transition from molecular physiology to pathophysiological relevance. *Am J Physiol Regul Integr Comp Physiol*. 2007;293:R568–R577.
41. Lerchenmuller C, Heissenberg J, Damilano F, Bezzeridis VJ, Kramer I, Bochaton-Piallat ML, Hirschberg K, Busch M, Katus HA, Peppel K, Rosenzweig A, Busch H, Boerries M, Most P. S100A6 regulates endothelial cell cycle progression by attenuating antiproliferative signal transducers and activators of transcription 1 signaling. *Arterioscler Thromb Vasc Biol*. 2016;36:1854–1867.
42. Stephanou A, Brar BK, Scarabelli TM, Jonassen AK, Yellon DM, Marber MS, Knight RA, Latchman DS. Ischemia-induced STAT-1 expression and activation play a critical role in cardiomyocyte apoptosis. *J Biol Chem*. 2000;275:10002–10008.
43. McCormick J, Suleman N, Scarabelli TM, Knight RA, Latchman DS, Stephanou A. STAT1 deficiency in the heart protects against myocardial infarction by enhancing autophagy. *J Cell Mol Med*. 2012;16:386–393.
44. Leong-Poi H, Kuliszewski MA, Lekas M, Sibbald M, Teichert-Kuliszewska K, Klibanov AL, Stewart DJ, Lindner JR. Therapeutic arteriogenesis by ultrasound-mediated VEGF165 plasmid gene delivery to chronically ischemic skeletal muscle. *Circ Res*. 2007;101:295–303.
45. Cao WJ, Rosenblat JD, Roth NC, Kuliszewski MA, Matkar PN, Rudenko D, Liao C, Lee PJ, Leong-Poi H. Therapeutic angiogenesis by ultrasound-mediated microRNA-126-3p delivery. *Arterioscler Thromb Vasc Biol*. 2015;35:2401–2411.
46. Fiedler J, Thum T. MicroRNAs in myocardial infarction. *Arterioscler Thromb Vasc Biol*. 2013;33:201–205.